ACS APPLIED MATERIALS & INTERFACES

Research Article

www.acsami.org

Carbon Nanoparticles Trapped in Vivo—Similar to Carbon Nanotubes in Time-Dependent Biodistribution

Jia-Hui Liu,[†,‡] Sheng-Tao Yang,*[,§] Xin Wang,[⊥] Haifang Wang,*[,†] Yamin Liu,[⊥] Pengju G. Luo,[⊥] Yuanfang Liu,[†,#] and Ya-Ping Sun*[,⊥]

[†]Institute of Nanochemistry and Nanobiology, Shanghai University, Shanghai 200444, China

[‡]Beijing Key Laboratory of Bioprocess, College of Life Science and Technology, Beijing University of Chemical Technology, Beijing 100029, China

[§]College of Chemistry and Environment Protection Engineering, Southwest University for Nationalities, Chengdu 610041, China

[⊥]Department of Chemistry and Laboratory for Emerging Materials and Technology, Clemson University, Clemson, South Carolina 29634-0973, United States, and

[#]Beijing National Laboratory for Molecular Sciences, College of Chemistry and Molecular Engineering, Peking University, Beijing 100871, China

ABSTRACT: Carbon nanoparticles are in all of the carbon nanomaterials that are presently widely pursued for potential bioapplications, but their in vivo biodistribution-related properties are largely unknown. In this work, highly ^{13}C-enriched carbon nanoparticles were prepared to allow their quantification in biological samples by using isotope-ratio mass spectroscopy. The in vivo biodistribution results are presented and discussed, and also compared with those of the aqueous suspended carbon nanotubes reported previously. The distribution profile and time dependencies are largely similar between the nanoparticles and nanotubes, with results on both suggesting meaningful accumulation in some major organs over an extended period of time. Therefore, the surface modification of carbon nanoparticles, preferably the chemical functionalization of the nanoparticles with biocompatible molecules or species, is desirable or necessary in the pursuit of these nanomaterials for various bioapplications.

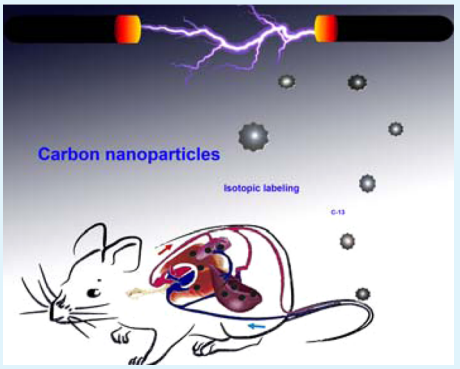

KEYWORDS: *carbon nanoparticles, biodistribution, carbon nanotubes, toxicity, ^{13}C labeling, isotope-ratio mass spectroscopy*

INTRODUCTION

Carbon nanomaterials have attracted much recent attention for their potential applications in biology and medicine.[1−3] Among the widely studied carbon nanomaterials, however, carbon nanoparticles almost always play a significant role, either as primary components or as residues or even unwanted yet unavoidable impurities. For example, samples of single-walled carbon nanotubes (SWNTs) after purification in various established methods generally still contain a significant amount of nanoscale carbonaceous materials,[1,4−6] which might be loosely considered as carbon nanoparticles. The presently extensively pursued graphene materials may also have carbon nanoparticles as impurities. In fact, purification methods for preparing pure carbon nanotubes or graphene sheets may even create nanoscale carbon particles as fragments from breaking up the targeted carbon nanomaterials under harsh processing conditions, such as in oxidative acid treatment with prolonged sonication.[7] More recently, carbon nanoparticles have been exploited as precursors for a new class of fluorescent nanomaterials, dubbed "carbon dots", which are generally defined as small carbon nanoparticles with various particle surface passivation.[8−16]

For potential bioapplications of carbon nanotubes, dots, or other nanomaterials, the properties and behavior of carbon nanoparticles in vitro and in vivo are of significant interest, as these particles are generally present in the samples as unavoidable impurities or the functionalized particles may become "naked" due to defunctionalization in metabolic or other processes.[17] There have been a few cytotoxicity studies of nanoscale carbon particles in recent years.[18−21] For example, Ray et al. evaluated the acid-purified carbon nanoparticles in MTT (3-(4,5-dimethylthiazol-2-yl)-2,5-diphenyltetrazolium bromide) and Typan blue assays with HepG2 cells and found no significant cytotoxicity.[18] Zhao et al. prepared carbon nanoparticles by electro-oxidation of graphite in aqueous solution, and examined and confirmed the biocompatibility of these nanoparticles with respect to 293T human kidney cells.[19] Liu et al. harvested nanoparticles from the carbon soot produced in arc-discharge of graphite rods, and refluxed the nanoparticles in aqueous nitric acid to induce oxidative moieties such as carboxylic acids onto the particle surface.[20] These

Received: June 22, 2014
Accepted: July 28, 2014
Published: July 28, 2014

carbon nanoparticles could be dispersed in aqueous solution for cytotoxicity evaluations, and the results suggested that the particles were nontoxic to human adenocarcinoma lung adenocarcinoma and human colorectal adenocarcinoma HT-29 cells.[20]

Small carbon nanoparticles with the particle surface functionalized with oligomeric poly(ethyelene glycol) have also been evaluated in vivo, for which the aqueous solution of the functionalized nanoparticles was injected into mice intravenously.[22] No significant toxic effects were observed, thus supporting the notion that well-functionalized and solubilized carbon nanomaterials are generally less toxic.[1,23] However, in light of the substantial difference in toxicity behavior between purified pristine carbon nanotubes and their soluble functionalized counterparts,[24−28] a determination on the biodistribution of naked small carbon nanoparticles in vivo should prove valuable in general, and in particular to the development of the recently widely pursued fluorescent carbon dots for bioapplications, as carbon nanoparticles are the cores in carbon dots.[3,8] In this work, we prepared highly ^{13}C-enriched carbon nanoparticles to allow their quantification in biological samples by using isotope-ratio mass spectroscopy. The in vivo biodistribution results are presented and discussed, and also compared with those of the aqueous suspended SWNTs reported previously.[24] There are apparently significant similarities between the nanoparticles and nanotubes in their in vivo distributions over the monitored time period (up to 28 days), with results on both suggesting meaningful accumulation in some major organs. The comparison has also helped to clarify some of the issues on the in vivo behavior of carbon nanotubes, such as the possibility with respect to crossing the blood brain barrier.

RESULTS AND DISCUSSION

Carbon soot with ^{13}C enrichment was produced in the arc discharge of graphite rods.[24] In the experiment, a solid graphite rod acquired commercially was used as the cathode, and the same kind of rod was modified for the use as the anode. The modification was such that the graphite rod was made hollow by using a driller, followed by filling the hollow cavity with a mixture of ^{13}C powders and carbon cement. Upon the completion of the arc discharge production, the carbon soot was harvested and processed in terms of vigorous sonication and refluxing in aqueous nitric acid, coupled with subsequent dialysis and centrifugation, to yield an aqueous suspension of small carbon nanoparticles with a substantial ^{13}C enrichment. With the stable suspension (Figure 1), optical absorption, and fluorescence measurements could readily be performed. Also shown in Figure 1 are the observed UV/vis absorption and fluorescence emission spectra of the aqueous suspended carbon nanoparticles.

The carbon nanoparticles in the aqueous suspension were generally small, less than 10 nm in average diameter, as confirmed by results from the atomic force microscopy (AFM) characterization (Figure 2) and transmission electron microscopy (TEM) imaging (Figure 3). The particles were found to be mostly amorphous in powder X-ray diffraction analyses and, as expected, to have substantial defects (likely on the particle surface) according to Raman results showing a relatively intense D-band (Figure 4). Because of the carbon nanoparticles being very small, their aqueous suspensions prepared from the vigorous centrifugation in a high-speed centrifuge (up to 390 000*g*) were solutionlike (Figure 1), stable with respect to the absence of any precipitation over an extended period of time (at least several months). The suspensions could be used directly in cytotoxicity assays, with the results showing no significant toxicities.[20]

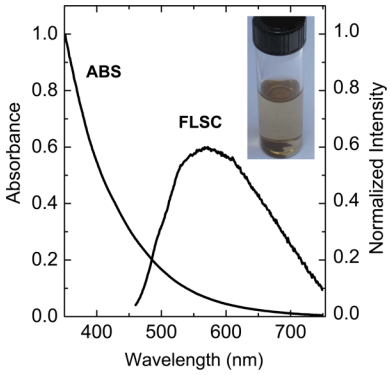

Figure 1. Absorption (ABS) and fluorescence (FLSC, 440 nm excitation) of the aqueous dispersed carbon nanoparticles. Inset: photo showing a typical stable aqueous dispersion.

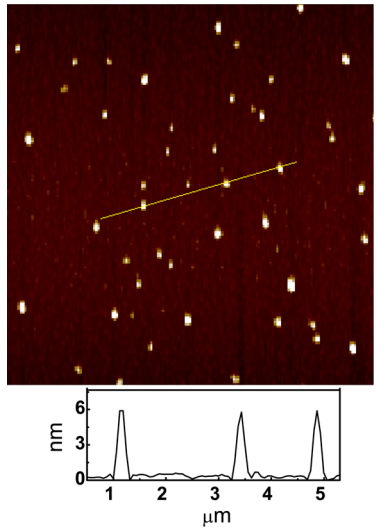

Figure 2. AFM images with height analysis results for the carbon nanoparticles on mica substrate.

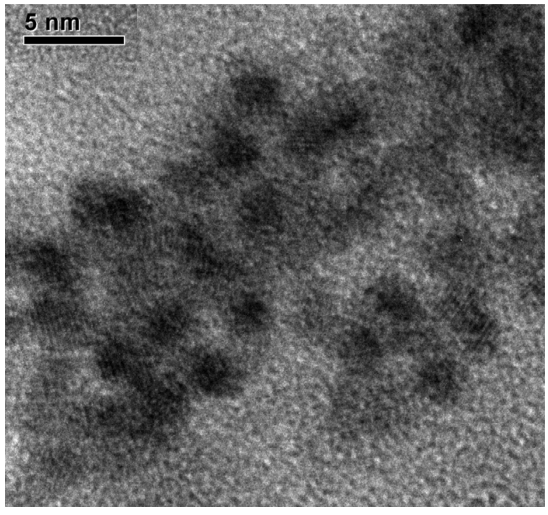

Figure 3. High-resolution TEM images of the carbon nanoparticles.

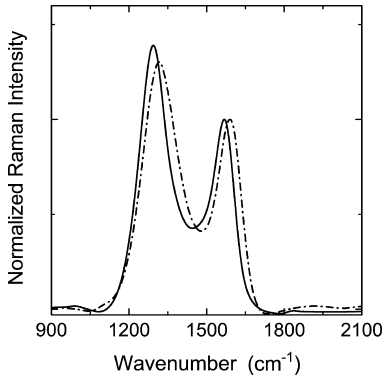

Figure 4. Raman G-band and D-band features of the ^{13}C-enriched carbon nanoparticles (solid line) shifted from those without the enrichment (dash-dot line).

The ^{13}C enrichment in carbon nanomaterials has been an effective way to allow quantification of the nanomaterials in organs and other biological systems by using isotope-ratio mass spectroscopy (MS).[24,26] In this study, a solutionlike aqueous suspension of the ^{13}C-enriched carbon nanoparticles was prepared, in which the ^{13}C content was determined by the MS method. For the isotope-ratio MS, a single focusing magnetic sector mass spectrometer with fixed multiple detectors (one per isotope) was used. The method generally requires the conversion of the sample being tested to simple molecules prior to the MS measurement. In this study specifically, the biological sample (an organ harvested from mice and then processed, for example) containing carbon nanoparticles was first converted to CO_2 and other species, and the ratio of $^{13}CO_2/^{12}CO_2$ was determined for the desired quantification.

In the experiment for in vivo biodistribution,[29,30] the stable aqueous suspension of the ^{13}C-enriched carbon nanoparticles was used for the intravenous injection into mice. Following the injection, the concentration of the nanoparticles in blood circulation was monitored over time (in terms of isotope-ratio MS analyses of ^{13}C), and the results suggested that the concentration decay in vivo was rather fast. It took about 6 h for the nanoparticles to be largely cleared from the bloodstream. This blood clearance rate for the nanoparticles was somewhat faster than that previously reported for the similarly purified SWNTs in aqueous suspension, even though in the nanotube case a surfactant was used to assist the dispersion of SWNTs and also the stabilization of the resulting aqueous suspension.[24] An argument here might be that the carbon nanoparticles were much smaller in size than the nanotubes. However, there were also a number of studies suggesting that smaller particles were slower in blood clearance than their larger counterparts, as the former could more effectively evade the reticuloendothelial system, and thus potentially longer intravascular retention, less macrophage activity, and/or reduced febrile responses.[31,32] For the comparison between nanoparticles and nanotubes discussed above, the shape of the nanoscale entities might be playing a significant role in the blood clearance rate. As for the effect of surface modification, the presence of surfactant molecules in the aqueous suspension of SWNTs might have distorted the intrinsic blood clearance behavior of the nanotubes. In the case of organic molecules on the surface of carbon nanoparticles, such as the chemical functionalization of the nanoparticles in brightly fluorescent carbon dots,[3] the effect on blood clearance is apparently less significant. For example, the PEGylated carbon dots exhibited similarly rapid blood clearance to that of the naked carbon nanoparticles discussed above, and in fact, the PEGylated carbon dots were found to nearly complete the renal secretion in less than 10 h.[33] It should be noted that naked nanomaterials are known to adsorb proteins in bloodstream (not naked anymore), with the same for the carbon nanoparticles. Although the effects are mechanistically complex, it is likely that the protein adsorption in blood triggers the phagocytic recognition and reticuloendothelial system (RES) capture of xenobiotics.[34]

The rapid clearance of the carbon nanoparticles from the blood steam facilitated their distributions throughout most of the organs in mice. The mice were sacrificed to collect the organs at various time points postexposure, up to 28 days. The accumulation levels of the carbon nanoparticles in major organs and tissues, including heart, liver, spleen, stomach, kidneys, lungs, intestine, and brain, were determined on the basis of quantitative ^{13}C isotopic measurements with the isotope-ratio MS. The biodistribution data thus obtained are shown in Figure 5. Apparently, lungs, spleen, and liver were the organs of

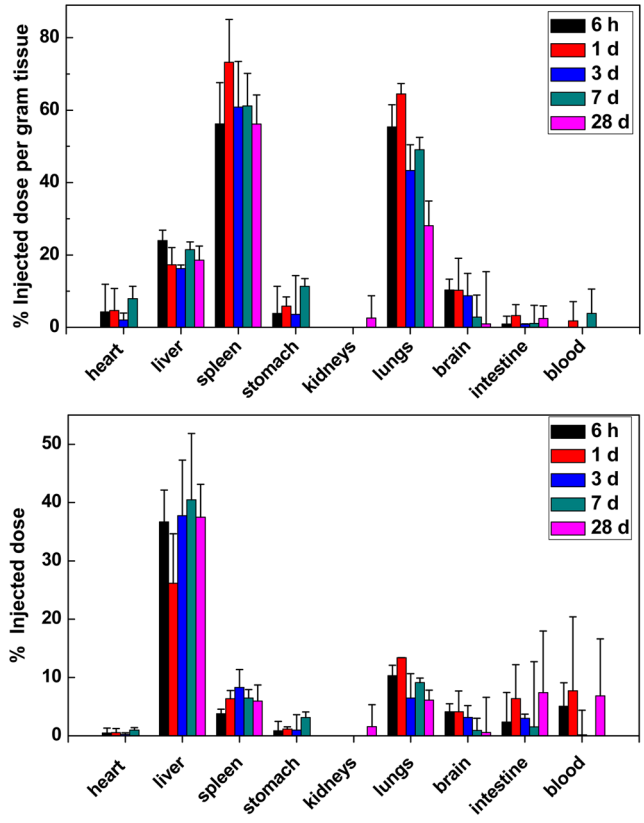

Figure 5. Biodistribution results (in the mean SD, n = 4) for the carbon nanoparticles in various organs of mice at different time points postexposure, presented as (top) the percentage of injected dose per gram tissue; and (bottom) the percentage of injected dose (thus emphasizing the weight of each organ).

primary accumulations (Table 1), similar to those found in the in vivo biodistribution study of aqueous dispersed SWNTs.[24] The average total accumulation level in these organs for the nanoparticles appeared as being higher than that for the nanotubes (Table 1), for which the presence of a dispersion agent (the surfactant Tween 80) in the aqueous suspended nanotubes might be considered.[24] However, with the relatively

Table 1. Percentage of Injected Dose (% ID) per Organ Values for the Carbon Nanoparticles in Major Organs at Different Time Points Are Compared with Those for SWNTs[a]

	liver		spleen		lungs	
	nanoparticles	SWNTs[a]	nanoparticles	SWNTs[a]	nanoparticles	SWNTs[a]
1 day	26.2 ± 8.5	21.1 ± 2.3	6.4 ± 1.4	1.2 ± 0.3	13.7 ± 0.0	15.0 ± 5.2
7 day	40.5 ± 11.4	18.5 ± 4.4	6.5 ± 1.4	1.6 ± 0.3	9.1 ± 0.7	13.3 ± 1.9
28 day	37.5 ± 5.6	21.9 ± 3.2	6.0 ± 2.8	1.8 ± 0.5	6.1 ± 1.7	9.4 ± 3.2

[a]With the presence of surfactant molecules on nanotubes for their dispersion (from ref 24).

large error margins of the data, the comparison should probably be characterized as being qualitatively similar. The similarity could also be found in the time dependencies of the accumulation between the carbon nanoparticles and nanotubes (Table 1).[24] The rapid uptake of the carbon nanoparticles was probably through the mononuclear phagocytes in the RES, which typically acts as mechanical filters to efficiently entrap particles in vivo.[35] The gradual clearance of the carbon nanoparticles from lungs over the 28-day observation period could be attributed to the particles being secreted by the alveolar macrophage as mucus through mucociliary transport to leave the lungs.[36]

In the literature, the general principle for particulates in vivo is such that those with diameters larger than two microns are trapped in pulmonary capillary vessel, while those between 100 nm and two microns in diameter are trapped by liver and spleen.[37,38] The carbon nanoparticles in this study were rather small, mostly on the order of 10 nm or less in diameter (Figures 2 and 3). Therefore, the observed primary accumulation in lungs would suggest some meaningful aggregation of the carbon nanoparticles in blood circulation, though the accumulation level was still lower than what was found for the similarly purified and aqueous suspended SWNTs.[24] The results more comparable with those of SWNTs[39] are such that the majority of the entrapped carbon nanoparticles were in the other two important organs in RES, spleen and liver. Even at 28 days postexposure, the accumulation level in spleen was still high at about 60% injected dose per gram tissue, and in liver about 20% injected dose per gram tissue (or about 37% of the total injected dose because of the large mass of liver, Figure 5). As for possible excretion pathways, one might be through the bile to feces,[40] and another for these relatively small particles to pass through kidneys to urine, similar to quantum dots.[41]

In the previous investigation on the in vivo biodistribution of the similarly purified and aqueous suspended SWNTs,[24] an intriguing finding was on the small amount of ^{13}C detected in brain tissue, raising the possibility that the nanotubes might be able to overcome the blood brain barrier. Despite the repeated electron microscopy search at the time, however, no carbon nanotubes were found in the brain tissue.[24] The results obtained in this work may prove largely negative to the possibility, as clearly detectable amounts of the carbon nanoparticles were in the brain tissues over the 28-day monitoring period, suggesting that the previous observation for the nanotube sample was more likely due to the contribution of nanoscale carbonaceous impurities (or carbon nanoparticles in particular).[24] Nevertheless, while not SWNTs, the confirmation here that the small carbon nanoparticles could overcome the blood brain barrier still represents an interesting finding with potentially significant implications, worthy of further exploration in future studies.

The in vivo behavior of carbon nanoparticles has largely been ignored, with only rather limited results available in the literature,[2,22,33,42,43] despite the extensive investigations on carbon nanotubes and more recently graphene materials and again for the fact that nanoparticles are almost always a part of the other carbon nanomaterials. A seemingly good news based on the results from this work is that there are major similarities in the in vivo biodistribution between carbon nanoparticles and nanotubes, allowing potentially the extrapolation of the available results from carbon nanotubes to nanoparticles. For the former, surface modification is known for its major effects, as highlighted in several recent reviews. For example, Ali-Boucetta and Kostarelos examined the important factors affecting the biodistribution and pharmacokinetic profile of carbon nanotubes following systemic, pulmonary, and dermal exposure and concluded that the quality of the dispersion, preferably through chemical functionalization, plays a critical role.[23] The good dispersion of carbon nanotubes as a result of chemical functionalization generally leads to significant and rapid urinary excretion, in contrast to the preferential and predominant accumulation of pristine or noncovalently coated nanotubes in RES organs (liver and spleen).[23] Al-Jamal et al. attributed the latter to possibly in vivo bundling of the nanotubes.[44] The results of carbon nanoparticles and their surface-functionalized counterparts[3,33] are generally similar to those of the pristine and functionalized nanotubes, respectively, except that for the nanoparticles without functionalization the presumably in vivo aggregation may be somewhat less dramatic because of the particle shape (vs the more severe bundling of carbon nanotubes). Nevertheless, naked carbon nanoparticles can be trapped to a significant extent and for an extended period of time in RES organs, suggesting the need for surface modification or functionalization and for the prevention of carbon dots from surface defunctionalization in various in vivo applications. This is particularly relevant to the apparent current divide between fluorescent carbon dots defined as small carbon nanoparticles with chemically functionalized particle surface and those of the nanoparticles only with some limited surface modification (such as the introduction of oxygen-containing surface moieties in this work) for the purpose of aqueous dispersion,[3,45] as the latter administered intravenously are more likely trapped in some major organs.

SUMMARY AND CONCLUSION

Aqueous dispersed small carbon nanoparticles were investigated for their biodistribution in vivo (mice) and time dependencies postexposure, with the results filling pretty much a void in the study of carbon nanomaterials for bioapplications, as the fact is that carbon nanoparticles are in all of the carbon nanomaterials. Similar to pristine carbon nanotubes, the carbon nanoparticles are captured by RES with significant accumulation levels in lungs, spleen, and liver. The distribution profile and time dependencies are also largely comparable (within experimental error margins) between the nanoparticles and

nanotubes, despite their obviously different shapes and overall sizes. Although the similarities might be useful in extrapolating the better known in vivo behavior of carbon nanotubes to that of the carbon nanoparticles, the same extrapolation of concerns on carbon nanotubes being trapped in major organs should also be considered. Therefore, the surface modification of carbon nanoparticles, preferably the chemical functionalization of the nanoparticles with biocompatible organic molecules for more fluorescent carbon dots, is desirable or necessary in the pursuit of these nanomaterials for various bioapplications.

EXPERIMENTAL SECTION

Materials. Amorphous ^{13}C powder (99.99% carbon, ^{13}C content >98%) was supplied by Icon Isotopes, and fine-extruded graphite rods (carbon content >99.9%) by Graphitestore.com, Inc. Carbon cement was obtained from Dylon Industries. Cellulose ester dialysis tubing with a molecular weight cutoff (MWCO) of 500 was purchased from Sigma.

Measurements. Baxter Megafuge (model 2630) and Beckman-Coulter ultracentrifuge (Optima L90K with a type 90 Ti fixed-angle rotor) were used for centrifugation at various *g* values. Crest Ultrasonics ultrasonic bath (model 950DA) operating in the range of 50−60 Hz was used in the dispersion of the nanoparticles. UV/vis absorption spectra were recorded on a Shimadzu UV2101-PC spectrophotometer. Fluorescence spectra were measured on a Jobin Yvon luminescence emission spectrometer equipped with a 450 W xenon source, a Gemini-180 excitation monochromator and a Tirax-550 emission monochromator, and a single-photon counting detector (Hamamatsu R928P PMT operated at 950 V). Atomic force microscopy (AFM) images were obtained in the acoustic AC mode on a Molecular Imaging PicoPlus AFM system equipped with a multipurpose scanner and a NanoWorld Point probe NCH sensor. The height profile analysis was assisted by using the SPIP software distributed by Image Metrology. The transmission electron microscopy (TEM) characterization was performed on an Hitachi H-9500 high-resolution TEM system. The quantification of ^{13}C content in various samples was accomplished by using a Sercon Integra CN isotope ratio mass spectrometer.

^{13}C-Enriched Carbon Nanoparticles. The carbon soot sample was produced in the arc-discharge of two graphite rods, one of which (the anode) was loaded with ^{13}C. For the preparation of the anode rod, a commercially supplied graphite rod was cut in half to ∼15 cm in length and then drilled to become hollow, with an inner diameter of ∼4 mm, and the hollow cavity was filled with a mixture of ^{13}C powders and carbon cement. The rod was annealed at 800 °C for 8 h in argon flow (50 sccm, atmospheric pressure). A solid graphite rod was used as cathode. The arc-discharge was carried out in a water-cooled stainless steel chamber equipped with an arc length controller (ALC-401, Jetline Engineering), under helium atmosphere (1 atm) and with a direct current of 70 A (28 V). The carbon soot on the chamber wall was collected.

The as-produced carbon soot enriched with ^{13}C was dispersed in dimethylformamide (DMF) with ultrasonication (Crest Ultrasonics, Model 950DA, 50−60 Hz) for 24 h, and the resulting suspension was evaporated to remove DMF for the carbon particles. The particle sample was refluxed in aqueous nitric acid solution (2.6 M) for 12 h. Upon being cooled to ambient, the acidic suspension was centrifuged at 3500*g* to collect the supernatant, which was then neutralized with sodium carbonate. The suspension was dialyzed (membrane MWCO ∼ 500) against fresh deionized water for 3 days, followed by centrifugation at 390 000*g* to obtain a stable dispersion of the ^{13}C-enriched carbon nanoparticles.

For the TEM characterization, an aliquot of the particle suspension was diluted. A few drops of the diluted aqueous suspension were deposited onto a silicon oxide-coated copper grid, followed by the removal of water via evaporation.

Biodistribution in Vivo. Male CD-1 mice (∼25 g) were purchased from Peking University Animal Center. The mice were cared by following established protocols in compliance with the Institutional Animal Care and Use Program Guidelines. After acclimation, the mice were randomly divided into groups of four each for the in vivo biodistribution study. Each mouse was exposed intravenously to ^{13}C-enriched carbon nanoparticles in a single injection of 200 μg carbon nanoparticles in 200 μL. Mice injected with 0.9% NaCl aqueous solution were taken as the control group.

At 6 h, 1 day, 3 days, 7 days, and 28 days post-exposure, the mice were sacrificed. The blood and tissue samples (including heart, liver, spleen, stomach, kidneys, lungs, brain, and intestine) were collected for ^{13}C abundance measurements. The samples were homogenized, lyophilized and grounded into fine powder. The quantification in terms of the ^{13}C isotopic abundance was performed on an isotope-ratio mass spectroscopy following the protocols already established in the literature. The δ value from isotope-ratio MS was converted into $^{13}C/^{12}C$ ratio (r) following eq 1, where the $^{13}C/^{12}C$ ratio of the VPDB standard sample $[(^{13}C/^{12}C)_{standard}]$ was 0.0112372. The r value was then calculated into percentage of ^{13}C in mass (ω_{13_C}) following eq 2. The amount of ^{13}C-enriched carbon nanoparticles in samples ($m_{13C-carbon\ nanoparticles}$) could be obtained from eq 3, where ω_{carbon} from isotope-ratio MS was the content of carbon in the dry sample, m_{sample} the sample weight, m_{dry} and m_{wet} the weights of tissue after and before drying, respectively. The ^{13}C content in the ^{13}C-enriched carbon nanoparticles was 15.78%.

$$r = \left(\frac{\delta}{1000} + 1\right)(^{13}C/^{12}C)_{standard} \quad (1)$$

$$\omega_{^{13}C} = \frac{r13}{r13 + 12}100\% \quad (2)$$

$$m_{^{13}C-carbon\ nanoparticles} = \frac{[\omega_{^{13}C}(sample) - \omega_{^{13}C}(control)]\left(\omega_{carbon} m_{sample}\frac{m_{dry}}{m_{wet}}\right)}{15.78\%} \quad (3)$$

The content of ^{13}C-enriched carbon nanoparticles in tissue samples can be expressed as %ID/g (percentage of injected dose per gram tissue, eq 4) and %ID (percentage of injected dose, eq 5), where the dose is the amount of injected ^{13}C-enriched carbon nanoparticles and m_{sample} denotes the weight of the tissue sample.

$$\%ID/g = \frac{m_{^{13}C-carbon\ nanoparticles}}{dose}100\%/m_{sample} \quad (4)$$

$$\%ID = \frac{m_{^{13}C-carbon\ nanoparticles}}{dose}100\% \quad (5)$$

AUTHOR INFORMATION

Corresponding Authors

*E-mail: yangst@pku.edu.cn.
*E-mail: hwang@shu.edu.cn.
*E-mail: syaping@clemson.edu.

Notes

The authors declare no competing financial interest.

ACKNOWLEDGMENTS

The work in China was supported by China Natural Science Foundation (21301015 for J.-H.L. and 21307101 for S.-T.Y.) and National Basic Research Program of China (973 Program, 2011CB933402 for H.W.). The effort at Clemson U. was supported by the National Science Foundation.

REFERENCES

(1) Lu, F.; Gu, L.; Meziani, M. J.; Wang, X.; Luo, P. G.; Veca, L. M.; Cao, L.; Sun, Y.-P. Advances in Bioapplications of Carbon Nanotubes. *Adv. Mater.* **2009**, *21*, 139−152.

(2) Wang, Y.; Li, Z.; Wang, J.; Li, J.; Lin, Y. Graphene and Graphene Oxide: Biofunctionalization and Applications in Biotechnology. *Trends Biotechnol.* **2011**, *29*, 205−212.
(3) Luo, P. G.; Yang, F.; Yang, S.-T.; Sonkar, S. K.; Yang, L. J.; Broglie, J. J.; Liu, Y.; Sun, Y.-P. Carbon-Based Quantum Dots for Fluorescence Imaging of Cells and Tissues. *RSC Adv.* **2014**, *4*, 10791−10807.
(4) Zhao, B.; Hu, H.; Niyogi, S.; Itkis, M. E.; Hamon, M. A.; Bhowmik, P.; Meier, M. S.; Haddon, R. C. Chromatographic Purification and Properties of Soluble Single-Walled Carbon Nanotubes. *J. Am. Chem. Soc.* **2001**, *123*, 11673−11677.
(5) Itkis, M. E.; Perea, D. E.; Niyogi, S.; Rickard, S. M.; Hamon, M. A.; Hu, H.; Zhao, B.; Haddon, R. C. Purity Evaluation of As-Prepared Single-Walled Carbon Nanotube Soot by Use of Solution-Phase Near-IR Spectroscopy. *Nano Lett.* **2003**, *3*, 309−314.
(6) Xu, X.; Ray, R.; Gu, Y.; Ploehn, H. J.; Gearheart, L.; Raker, K.; Scrivens, W. A. Electrophoretic Analysis and Purification of Fluorescent Single-Walled Carbon Nanotube Fragments. *J. Am. Chem. Soc.* **2004**, *126*, 12736−12737.
(7) Musumeci, A. W.; Waclawik, E. R.; Frost, R. L. A Comparative Study of Single-Walled Carbon Nanotube Purification Techniques Using Raman Spectroscopy. *Spectrochim. Acta, Part A* **2008**, *71*, 140−142.
(8) Sun, Y.-P.; Zhou, B.; Lin, Y.; Wang, W.; Fernando, K. A. S.; Pathak, P.; Meziani, M. J.; Harruff, B. A.; Wang, X.; Wang, H.; Luo, P. G.; Yang, H.; Kose, M. E.; Chen, B.; Veca, L. M.; Xie, S.-Y. Quantum-Sized Carbon Dots for Bright and Colorful Photoluminescence. *J. Am. Chem. Soc.* **2006**, *128*, 7756−7757.
(9) Cao, L.; Wang, X.; Meziani, M. J.; Lu, F.; Wang, H.; Luo, P. G.; Lin, Y.; Harruff, B. A.; Veca, L. M.; Murray, D.; Xie, S.-Y.; Sun, Y.-P. Carbon Dots for Multiphoton Bioimaging. *J. Am. Chem. Soc.* **2007**, *129*, 11318−11319.
(10) Bourlinos, A. B.; Stassinopoulos, A.; Anglos, D.; Zboril, R.; Karakassides, M.; Giannelis, E. P. Surface Functionalized Carbogenic Quantum Dots. *Small* **2008**, *4*, 455−458.
(11) Peng, H.; Travas-Sejdic, J. Simple Aqueous Solution Route to Luminescent Carbogenic Dots from Carbohydrates. *Chem. Mater.* **2009**, *21*, 5563−5565.
(12) Li, H.; He, X.; Kang, Z.; Huang, H.; Liu, Y.; Liu, J.; Lian, S.; Tsang, C. H. A.; Yang, X.; Lee, S.-T. Water-Soluble Fluorescent Carbon Quantum Dots and Photocatalyst Design. *Angew. Chem., Int. Ed.* **2010**, *49*, 4430−4434.
(13) Li, Q.; Ohulchanskyy, T. Y.; Liu, R.; Koynov, K.; Wu, D.; Best, A.; Kumar, R.; Bonoiu, A.; Prasad, P. N. Photoluminescent Carbon Dots as Biocompatible Nanoprobes for Targeting Cancer Cells in Vitro. *J. Phys. Chem. C* **2010**, *114*, 12062−12068.
(14) Chandra, S.; Das, P.; Bag, S.; Laha, D.; Pramanik, P. Synthesis, Functionalization and Bioimaging Applications of Highly Fluorescent Carbon Nanoparticles. *Nanoscale* **2011**, *3*, 1533−1540.
(15) Li, H.; Kang, Z.; Liu, Y.; Lee, S.-T. Carbon Nanodots: Synthesis, Properties and Applications. *J. Mater. Chem.* **2012**, *22*, 24230−24253.
(16) Zhang, X.; Wang, S.; Zhu, C.; Liu, M.; Ji, Y.; Feng, L.; Tao, L.; Wei, Y. Carbon-dots Derived from Nanodiamond: Photoluminescence Tunable Nanoparticles for Cell Imaging. *J. Colloid Interface Sci.* **2013**, *397*, 39−44.
(17) Yang, S.-T.; Wang, H.; Meziani, M. J.; Liu, Y.; Wang, X.; Sun, Y.-P. Biodefunctionalization of Functionalized Single-Walled Carbon Nanotubes in Mice. *Biomacromolecules* **2009**, *10*, 2009−2012.
(18) Ray, S. C.; Saha, A.; Jana, N. R.; Sarkar, R. Fluorescent Carbon Nanoparticles: Synthesis, Characterization, and Bioimaging Application. *J. Phys. Chem. C* **2009**, *113*, 18546−18551.
(19) Zhao, Q. L.; Zhang, Z. L.; Huang, B. H.; Peng, J.; Zhang, M.; Pang, D. W. Facile Preparation of Low Cytotoxicity Fluorescent Carbon Nanocrystals by Electrooxidation of Graphite. *Chem. Commun.* **2008**, 5116−5118.
(20) Liu, J.-H.; Anilkumar, P.; Cao, L.; Wang, X.; Yang, S.-T.; Luo, P. G.; Wang, H.; Lu, F.; Meziani, M. J.; Liu, Y.; Korch, K.; Sun, Y.-P. Cytotoxicity Evaluations of Fluorescent Carbon Nanoparticles. *Nano LIFE* **2010**, *1*, 153−161.
(21) Kumar, P.; Meena, R.; Paulraj, R.; Chanchal, A.; Verma, A. K.; Bohidar, H. B. Fluorescence Behavior of Non-Functionalized Carbon Nanoparticles and Their in Vitro Applications in Imaging and Cytotoxic Analysis of Cancer Cells. *Colloids Surf., B* **2012**, *91*, 34−40.
(22) Yang, S.-T.; Wang, X.; Wang, H.; Lu, F.; Luo, P. G.; Cao, L.; Meziani, M. J.; Liu, J.-H.; Liu, Y.; Chen, M.; Huang, Y.; Sun, Y.-P. Carbon Dots as Nontoxic and High-Performance Fluorescence Imaging Agents. *J. Phys. Chem. C* **2009**, *113*, 18110−18114.
(23) Ali-Boucetta, H.; Kostarelos, K. Pharmacology of Carbon Nanotubes: Toxicokinetics, Excretion and Tissue Accumulation. *Adv. Drug Delivery Rev.* **2013**, *65*, 2111−2119.
(24) Yang, S.-T.; Guo, W.; Lin, Y.; Deng, X.-Y.; Wang, H. F.; Sun, H.-F.; Liu, Y.; Wang, X.; Wang, W.; Chen, M.; Huang, Y. P.; Sun, Y.-P. Biodistribution of Pristine Single-Walled Carbon Nanotubes in Vivo. *J. Phys. Chem. C* **2007**, *111*, 17761−17764.
(25) Lacerda, L.; Ali-Boucetta, H.; Herrero, M. A.; Pastorin, G.; Bianco, A.; Prato, M.; Kostarelos, K. Tissue Histology and Physiology Following Intravenous Administration of Different Types of Functionalized Multiwalled Carbon Nanotubes. *Nanomedicine (London, U. K.)* **2008**, *3*, 149−161.
(26) Yang, S.-T.; Fernando, K. A. S.; Liu, J.-H.; Wang, J.; Sun, H.-F.; Liu, Y.; Chen, M.; Huang, Y.; Wang, X.; Wang, H.; Sun, Y.-P. Covalently Pegylated Carbon Nanotubes with Stealth Character in Vivo. *Small* **2008**, *4*, 940−944.
(27) Bhirde, A. A.; Patel, S.; Sousa, A. A.; Patel, V.; Molinolo, A. A.; Ji, Y.; Leapman, R. D.; Gutkind, J. S.; Rusling, J. F. Distribution and Clearance of PEG-Single-Walled Carbon Nanotube Cancer Drug Delivery Vehicles in Mice. *Nanomedicine (London, U. K.)* **2010**, *5*, 1535−1546.
(28) Tabet, L.; Bussy, C.; Setyan, A.; Simon-Deckers, A.; Rossi, M. J.; Boczkowski, J.; Lanone, S. Coating Carbon Nanotubes with a Polystyrene-Based Polymer Protects against Pulmonary Toxicity. *Part. Fibre Toxicol.* **2011**, *8*, 3.
(29) Zhang, X.; Yin, J.; Kang, C.; Li, J.; Zhu, Y.; Li, W.; Huang, Q.; Zhu, Z. Biodistribution and Toxicity of Nanodiamonds in Mice after Intratracheal Instillation. *Toxicol. Lett.* **2010**, *198*, 237−243.
(30) Zhang, X.; Yin, J.; Peng, C.; Hu, W.; Zhu, Z.; Li, W.; Fan, C.; Huang, Q. Distribution and Biocompatibility Studies of Graphene Oxide in Mice after Intravenous Administration. *Carbon* **2011**, *49*, 986−995.
(31) Qi, K.; Al-Haideri, M.; Seo, T.; Carpentier, Y.; Deckelbaum, R. Effects of Particle Size on Blood Clearance and Tissue Uptake of Lipid Emulsions with Different Triglyceride Compositions. *J. Parenter. Enteral Nutr.* **2003**, *27*, 58−64.
(32) Keipert, P. E.; Otto, S.; Flaim, S. F.; Weers, J. G.; Schutt, E. A.; Pelura, T. J.; Klein, D. H.; Yaksh, T. L. Influence of Perflubron Emulsion Particle-Size on Blood Half-Life and Febrile Response in Rats. *Artif. Cells, Blood Substitutes, Immobilization Biotechnol.* **1994**, *22*, 1169−1174.
(33) Yang, S.-T.; Cao, L.; Luo, P. G.; Lu, F.; Wang, X.; Wang, H.; Meziani, M. J.; Liu, Y.; Qi, G.; Sun, Y.-P. Carbon Dots for Optical Imaging in Vivo. *J. Am. Chem. Soc.* **2009**, *131*, 11308−11309.
(34) Yang, S.-T.; Liu, Y.; Wang, Y.; Cao, A. Biosafety and Bioapplication of Nanomaterials by Designing Protein-Nanoparticle Interactions. *Small* **2013**, *9*, 1635−1653.
(35) Kutscher, H. L.; Chao, P.; Deshmukh, M.; Singh, Y.; Hu, P.; Joseph, L. B.; Reimer, D. C.; Stein, S.; Laskin, D. L.; Sinko, P. J. Threshold Size for Optimal Passive Pulmonary Targeting and Retention of Rigid Microparticles in Rats. *J. Controlled Release* **2010**, *143*, 31−37.
(36) Deng, X.; Jia, G.; Wang, H.; Sun, H.; Wang, X.; Yang, S.; Wang, T.; Liu, Y. Translocation and Fate of Multi-Walled Carbon Nanotubes in Vivo. *Carbon* **2007**, *45*, 1419−1424.
(37) Litzinger, D. C.; Buiting, A. M. J.; van Rooijen, N.; Huang, L. Effect of Liposome Size on the Circulation Time and Intraorgan Distribution of Amphipathic Poly(Ethylene Glycol)-Containing Liposomes. *Biochim. Biophys. Acta, Biomembr.* **1994**, *1190*, 99−107.

(38) Pettit, D. K.; Gombotz, W. R. The Development of Site-Specific Drug-Delivery Systems for Protein and Peptide Biopharmaceuticals. *Trends Biotechnol.* **1998**, *16*, 343−349.
(39) Liu, J.-H.; Yang, S.-T.; Wang, H.; Liu, Y. Advances in Biodistribution Study and Tracing Methodology of Carbon Nanotubes. *J. Nanosci. Nanotechnol.* **2010**, *10*, 8469−8481.
(40) Deng, X.; Jia, G.; Wang, H.; Sun, H.; Wang, X.; Yang, S.-T.; Wang, T.; Liu, Y. Translocation and Fate of Multi-walled Carbon Nanotubes in Vivo. *Carbon* **2007**, *45*, 1419−1424.
(41) Choi, H. S.; Liu, W.; Misra, P.; Tanaka, E.; Zimmer, J. P.; Ipe, B. I.; Bawendi, M. G.; Frangioni, J. V. Renal Clearance of Quantum Dots. *Nat. Biotechnol.* **2007**, *25*, 1165−1170.
(42) Tao, H.; Yang, K.; Ma, Z.; Wan, J.; Zhang, Y.; Kang, Z.; Liu, Z. In Vivo NIR Fluorescence Imaging, Biodistribution, and Toxicology of Photoluminescent Carbon Dots Produced from Carbon Nanotubes and Graphite. *Small* **2012**, *8*, 281−290.
(43) Bourdon, J. A.; Saber, A. T.; Halappanavar, S.; Jackson, P. A.; Wu, D. M.; Hougaard, K. S.; Jacobsen, N. R.; Williams, A.; Vogel, U.; Wallin, H.; Yauk, C. L. Carbon Black Nanoparticle Intratracheal Installation Results in Large and Sustained Changes in the Expression of Mir-135b in Mouse Lung. *Environ. Mol. Mutagen.* **2012**, *53*, 462−468.
(44) Al-Jamal, K.; Nunes, A.; Methven, L.; Ali-Boucetta, H.; Li, S.; Toma, F. M.; Herrero, M. A.; Al-Jamal, W. T.; ten Eikelder, H. M. M.; Foster, J.; Mather, S.; Prato, M.; Bianco, A.; Kostarelos, K. Degree of Chemical Functionalization of Carbon Nanotubes Determines Tissue Distribution and Excretion Profile. *Angew. Chem., Int. Ed.* **2012**, *51*, 6389−6393.
(45) Luo, P. G.; Sahu, S.; Yang, S.-T.; Sonkar, S. K.; Wang, J.; Wang, H.; LeCroy, G. E.; Cao, L.; Sun, Y.-P. Carbon ″Quantum″ Dots for Optical Bioimaging. *J. Mater. Chem. B* **2013**, *1*, 2116−2127.